Effect of lignin acetylation on the mechanical properties of lignin-poly-lactic acid biocomposites for advanced applications

Matilda Johansson [a], Mikael Skrifvars [a,*], Nawar Kadi [b], Hom Nath Dhakal [c]

[a] Swedish Centre for Resource Recovery, University of Borås, Borås 510 90, Sweden
[b] Department of Textile Technology, Faculty of Textiles, Engineering and Business, University of Borås, SE-501 90 Borås, Sweden
[c] Advanced Polymers and Composites (APC) Research Group, School of Mechanical and Design Engineering, University of Portsmouth, Portsmouth, Hampshire PO1 3DJ, UK

ARTICLE INFO

ABSTRACT

Bioplastics that possess characteristics like durability and low cost are desired for versatile applications in industries such as automotive manufacturing, marine transport manufacturing, aerospace applications, and the building industry. The automotive industry is an example of an industry that is now shifting towards a more focused approach addressing the issue concerning sustainability and the development of sustainable material. To achieve a lightweight and sustainable construction, one of the methods used by the automotive original equipment manufacturers is by substituting conventional fossil-based, non-renewable composites, and metallic materials with a bio-based alternative. One of the drawbacks with biobased polymers can be the poor interfacial adhesion, leading to poor mechanical properties when compares to conventional material. The aim of this research is to investigate if a low-cost by-product could be used as a component in a composite matrix material in the automotive industry to reduce the final weight and increase the non-petrochemical material usage of composite material without compromising the thermal and mechanicals properties demanded. In this research, lignin was chemically altered by esterification the functional groups to increase the compatibility with polylactic acid. The esterification was performed with the use of acetic acid anhydride and pyridine. To evaluate and determine the esterification, Fourier transform Infrared Spectroscopy was used. By blending the modified lignin with polylactic acid the intention was to improve the thermomechanical properties and the interfacial linkage between the components. The effects of lignin acetylation on the tensile properties, impact strength, and thermal stability and moisture repellence behaviour were investigated. According to the experimental results the modification of lignin, increased the impact strength for all the blends containing acetylated lignin compares to pristine lignin. The largest increase observed was for blends containing 20 wt% acetylated lignin and polylactic acid, which resulted in a 74% improvement compared with the blend composed of pristine lignin and polylactic acid. Similarly, the thermal stability was improved significantly with acetylation of the lignin. Moreover, the moisture repellence behaviour was also increased. The reason for the improved properties can be explained by the better interfacial compatibility between lignin and polylactic acid matrix. An increased thermal stability and a moisture repellent behaviour of the blends containing chemically modified lignin could be observed when compared with neat polylactic acid which makes the acetylation treatment of lignin a possible approach for the future of biocomposite production.

1. Introduction

Chemically derived polymers have been used to manufacture a variety of materials such as elastomers, man-made synthetic fibres, polymers, and plastic materials for many decades. The customization possibilities of these types of materials are extensive and so are the application areas intended for them as well. The chemically derived polymer materials have been tailored to the extent that they could be used as a replacement for conventional glass-based and metallic materials due to the cost effectiveness and high accessibility. However, due to an increasing interest in environmental and economic sustainability and a depletion of petroleum resources, the innovation of novel materials

Table 1
Conditions used in the extrusion process of blends containing PLA and lignin. Temperature zones (1–4) refers to the extruder sections from the feed section (zone 1) to the die (zone 4).

PLA/lignin composition (wt% ratio)	Zone 1 °C	Zone 2 °C	Zone 3 °C	Zone 4 °C	Retention time (min)	Screw speed (Rpm) Feeding/ mixing
95:5–70:30	200	200	200	180	3	75/125
60:40–40:60	200	200	200	180	5	75/150

Table 2
Conditions used in the injection moulding process of blends containing PLA and lignin. Steps refers to start, inject, and hold.

PLA/lignin composition (w/w)	Step 1 (Bar/Sec)	Step 2 (Bar/Sec)	Step 3 (Bar/Sec)	Cooling (°C)
95:5–40:60	10/2	12/5	12/10	25

derived from biologically renewable sources has become a main research topic. (Fernandes et al., 2013; Tamsilian et al., 2021). Renewable materials made from biological sources are currently being utilized in various industries, especially in the automotive and the bio-medical sector (Thakur et al., 2010). Two of the most commonly required properties for materials used in these industries are often to have both great strength and toughness to meet the rigorous performance demanded by the industry, however, the combinations of the two, are often hard to find in one material. Varied efforts have been targeted to convert biologically renewable materials, such as agricultural waste streams, to polymers, to create material that is biodegradable and sustainable. Majority of previous research works have been directed towards the utilization of natural fibres - as a reinforcing agent in polymer composites, but the research on lignin based polymer composites are still limited compared with cellulose (Thakur et al., 2014).

This vastly branched polyphenolic macromolecule is an abundant biopolymer available in nature, it is consisting of coniferyl, sinapyl and coumaryl alcohols linked together in an unstructured matter. The structure of lignin varies, depending on the origin of the biomass, which period it was harvested and which process was used for extraction (Lu et al., 2020; Yao et al., 2021). This biopolymer exist in all terrestrial plants and some aquatic organisms (Wang et al., 2016). It contributes to the structural strength and stiffness of vascular plant by acting as matrix for the cellulosic fibers. Lignin has previously generally been observed as a waste by-product in the pulping industry and has typically been combusted for energy in the pulping mills. Lignin is an extensively accessible and can be regenerated worldwide in significant amounts every year for use in carbon-neutral applications. There is an increasing interest in developing reliable and practical approaches for lignin utilization due to the scarcity of petroleum resources and the increased awareness regarding sustainability which results in an increasing demand for sustainable materials (Liao et al., 2020; Sameni et al., 2018). Although lignin has been studied for decades and shows great possibilities for biocomposites manufacturing, the drawbacks such as variety in quality and poor interfacial adhesion have to be handled to enable a large-scale production. Due to the hydroxyl groups in the macromonomer chains, lignin is poorly miscible with the majority of organic solvents and poorly compatible with chemically derived polymers. The result of the poor interfacial adhesion and poor miscibility with organic solvents in combination with a strong hydrogen bonding is agglomeration of lignin particles in the polymer matrix. If lignin could be modified to obtain thermoplastic properties many novel polymer materials and composites could be introduced (Parit and Jiang, 2020). The most common utilization path for lignin isolated from industrial waste streams is by energy recovery to fuel the inhouse production. Today only a small volume of the lignin fraction is valorized into specific product manufacturing ((Lora and Glasser, 2002; Sameni et al., 2018). Although
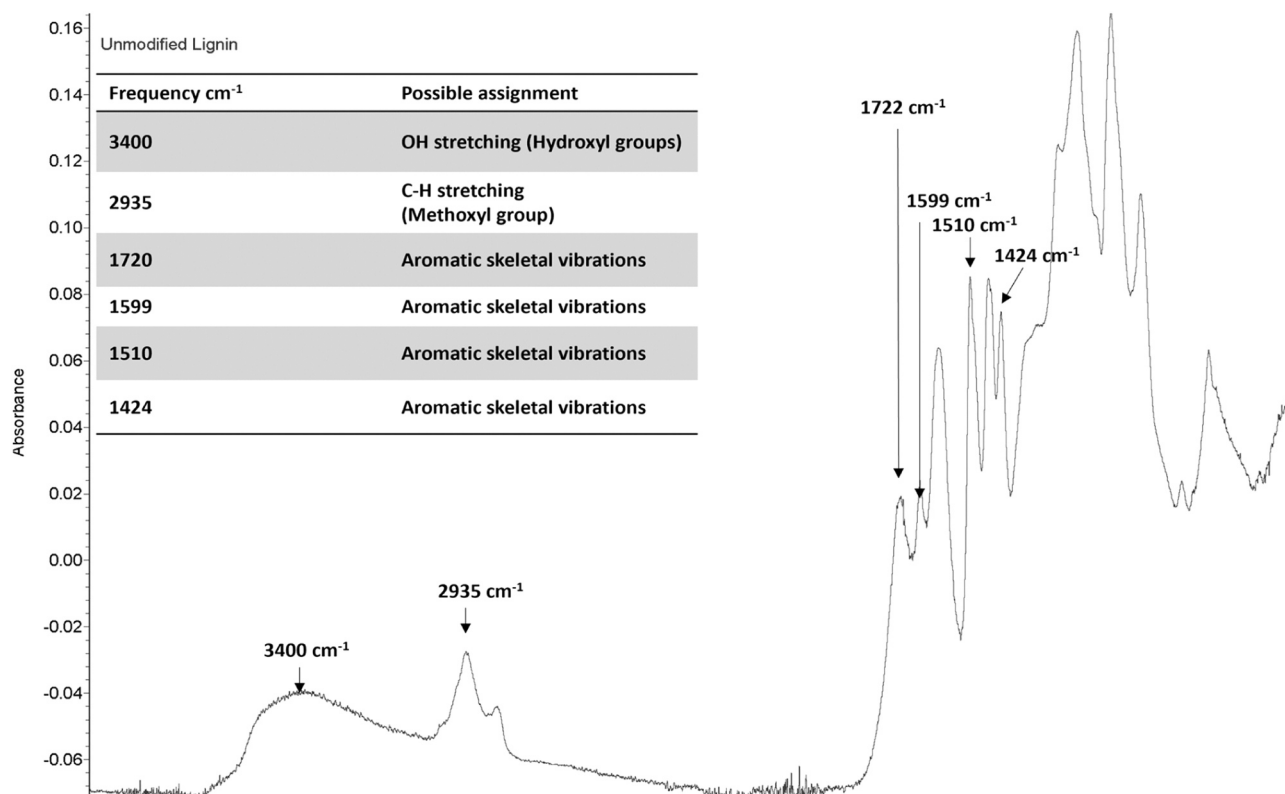

Unmodified Lignin	
Frequency cm⁻¹	**Possible assignment**
3400	OH stretching (Hydroxyl groups)
2935	C-H stretching (Methoxyl group)
1720	Aromatic skeletal vibrations
1599	Aromatic skeletal vibrations
1510	Aromatic skeletal vibrations
1424	Aromatic skeletal vibrations

Fig. 1. A) FTIR spectra of unmodified lignin. B) FTIR spectra of modified lignin.

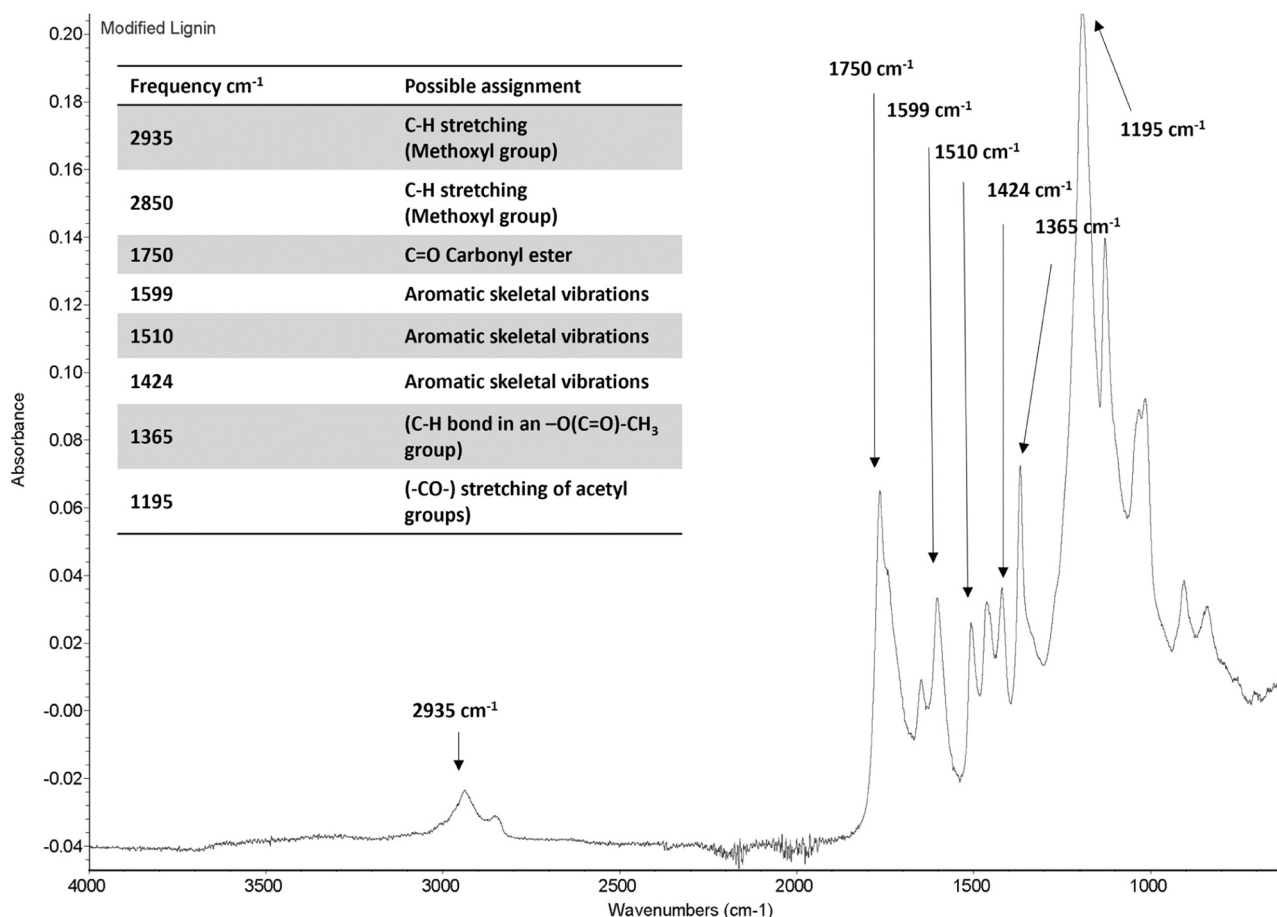| Frequency cm⁻¹	Possible assignment
2935	C-H stretching (Methoxyl group)
2850	C-H stretching (Methoxyl group)
1750	C=O Carbonyl ester
1599	Aromatic skeletal vibrations
1510	Aromatic skeletal vibrations
1424	Aromatic skeletal vibrations
1365	(C-H bond in an −O(C=O)-CH₃ group)
1195	(-CO-) stretching of acetyl groups)

Fig. 2. Tensile strength of neat PLA and PLA/lignin blends containing 5–60 wt.-% lignin.

it is available from the pulp and paper industry as a by-product, it is still often inadequately valorized (Ragauskas et al., 2014). Lignin derived from the pulping industry have been extensively characterized, however, for bio-refineries the detailed understanding regarding the lignin is still inadequate. The phenolic hydroxyl, the carboxyl, and methoxy groups in lignin could be modified to induce better compatibility with a wide collection of polymers. A broad research involving lignin have been conducted over the past decades and examples of application areas such as automotive component manufacturing, biomass for bioplastic production, adhesives and even antimicrobial agent for packaging, and cosmetic applications have been evaluated. (Agustiany et al., 2022). However, commercial production of lignin-based products are in need of more research and development. Some of the known drawbacks of bio derived polymers are poor interfacial adhesion with chemically derived polymers, the wide variation in purity due to the high dependence on origin, and extraction process leads to challenges in processing of the material and will hence, limit the application area of the biocomposites (Sameni, 2018). Because of the aromatic structure and the high carbon content, lignin could be a contender for biocomposites production. The structure complexity, however, makes a direct use of lignin difficult and to tackle this there is need for a chemical modification. Generally, chemical modification entails lignin de-polymerization, introduction of the other reactive sites, and functionalization of the hydroxyl groups (Figueiredo et al., 2018). Further development of the chemical modification routes, such as acetylation, esterification, and phenolation have been described previously (Taleb et al., 2020). Early attempts of lignin utilization resulted in increased stiffness and reduced tensile strength, and elongation compared with the neat polymer. These observations were ascribed to the inadequate adhesion between the polar lignin and the non-polar polymer. The lignin particles were assumed to agglomerate and act as stress concentration points in the matrix and therefore limits the application for unmodified lignin. The polymer used in this study was polypropylene (Pucciariello et al., 2004). Lignin have recently been discussed in literature when focusing on 3D-printing materials. In a study conducted by Tanase-Opedal et al., they concluded that lignin demonstrated the potential of being a suitable component for biocomposites materials appropriate for 3D-printing processes (Tanase-Opedal et al., 2019). In addition, a study to increase the printability of lignin based composites were conducted successfully (Nguyen et al., 2018). In other recent research focused on lignin valorization there have been reports of lignin composite material for electrochemical energy materials such as battery materials and supercapacitors where the authors state that lignin could be considered as a promising biopolymer for high performance battery systems, however, they also state that in order to full utilize lignin for this purpose there are still practical challenges to overcome (Culebras et al., 2019; Zhu et al., 2020). The most efficient technique to improve fuel economy and reduce emissions from a vehicle is by reducing the weight of the vehicle. New regulatory standards have been one of the driving forces for manufacturers to seek for new solutions to this problem (Park et al., 2015). In an attempt to partially substitute petroleum-based polyols, 15 different lignin types were investigated by Gondaliya and Nejad (2021) in the production of polyurethane flexible foams for automotive applications is was observed that organosolv lignin appeared to be more suitable for partial replacement of petrochemical polymers conventionally used foam production (Gondaliya and Nejad, 2021). The interest in research focusing on lignin valorization is on the rise (Agustiany et al., 2022; Anugwom et al., 2019; Collins et al., 2019; Triwulandari et al., 2019) but there are still challenges to overcome to reach the full potential of lignin.
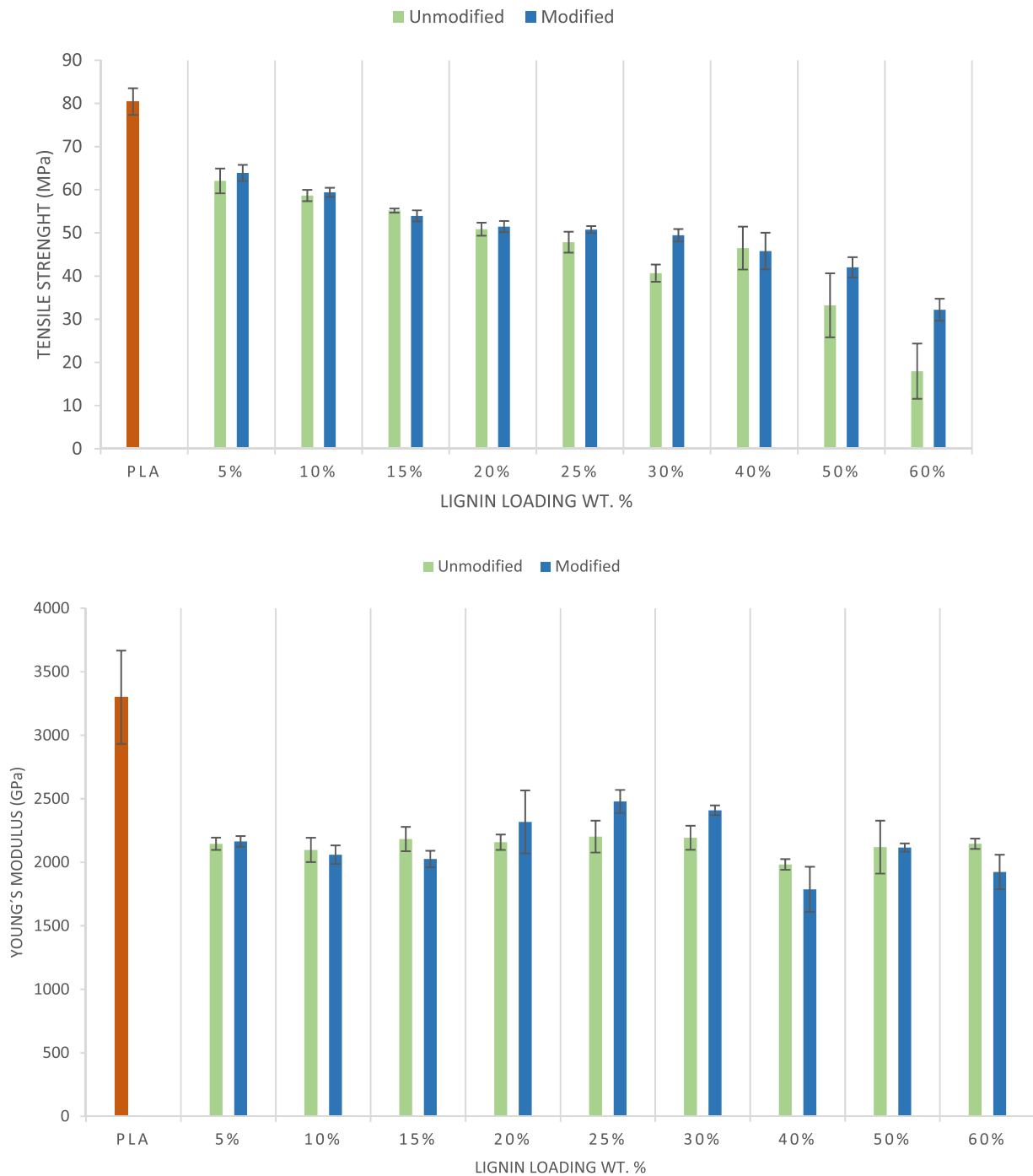
Fig. 3. Young's modulus of neat PLA and PLA/lignin blends containing 5–60 wt.-% lignin.

In this research, lignin was chemically altered by esterification the functional groups to enhance the compatibility with polymers such as, in this study, Polylactic acid (PLA) (Gordobil et al., 2014). There are a variety of paths to take to be able chemically modify lignin. One of the more commonly used method is esterification. To enhance the solubility of lignin, acetylation is a routine process (Wang, 2016). The length increase in carbon ester chains could result in an increase in tensile strength. Chemical modification of lignin reduces the polarity due to the esterification of the hydroxyl groups (Dehne et al., 2016). To increase the hydrophobic character and enhance the interfacial adhesion with PLA, the lignin was esterified using acetic anhydride. Acetylated lignin have also been reported to enhance the UV protection properties of a material (Kim et al., 2017). Incorporating hydrophobized lignin into

PLA blends may help to address the thermomechanical drawbacks, improve interfacial adhesion, and minimize the accumulation of lignin particles that has previously been observed in PLA blends with pristine lignin. Higher lignin loadings could result in improved material characteristics if modified lignin is used in PLA blends. In a previous study conducted by Yao and co-workers it was reported that the mechanical performance was able to be maintained at as high as 30 wt% of acetylated lignin (Yao et al., 2021).

Components fabricated using non-renewable conventional fibre such as glass are heavy as well inferior in toughness properties. Bio-composites reinforced with lignin not only provide light weight components, but this group of materials offer improved specific mechanical performance and sustainability compared to glass fibre composites.
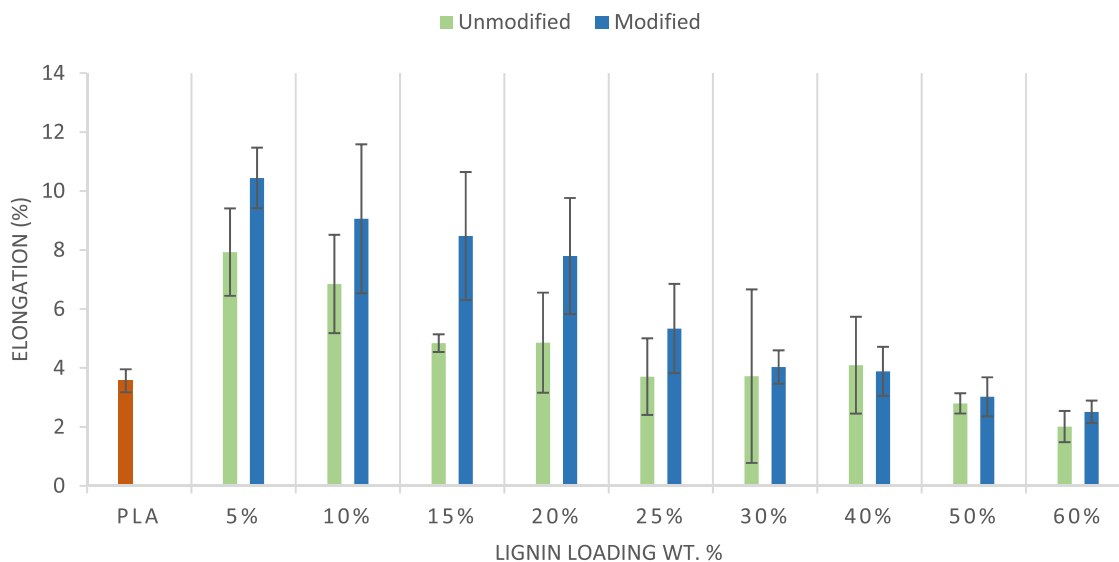
Fig. 4. Elongation of neat PLA and PLA/lignin blends containing 5–60 wt.-% lignin.
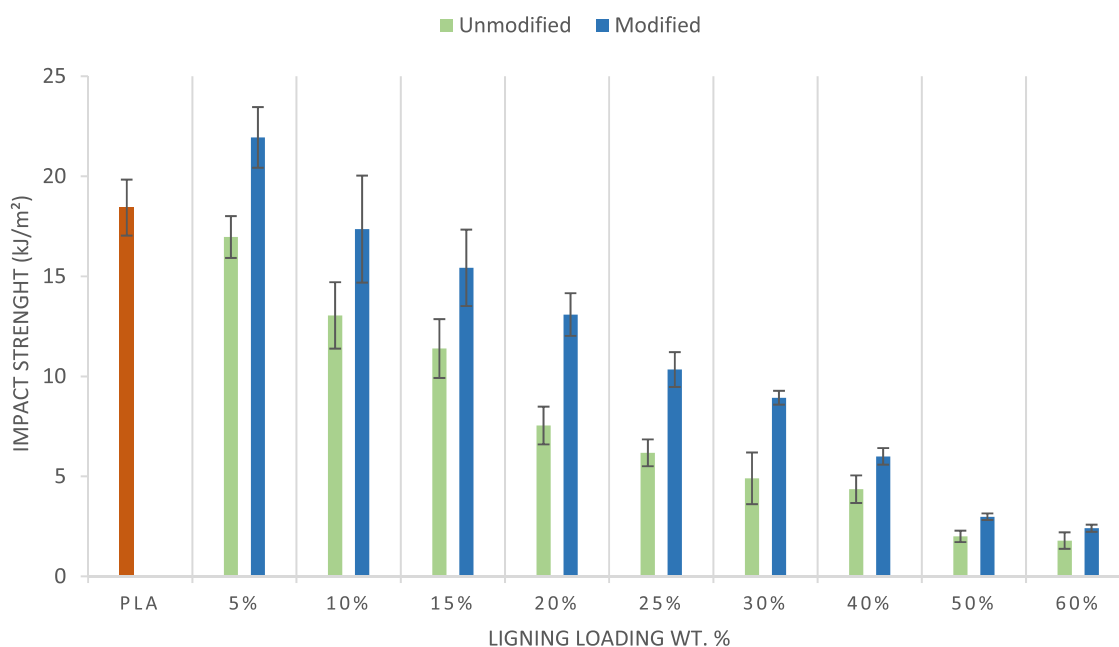

Fig. 5. Energy absorbed by un-notched Charpy impact tested samples.

Thus, the novelty aspects of this study lie in the development of fully green composites based on abundant renewable sources such as lignin, reinforced onto the PLA matrix.

This study intents to investigate the mechanical properties and moisture absorbance behavior of pristine lignin as well as acetylated lignin when blended with PLA. The aim of this work is the development of a thermoplastic bio-composite by utilizing bio-derived materials and waste streams to produce a lightweight material containing sustainable and biologically derived components suitable for advanced applications to reduce the ecological footprint and support a circular economy aspiration.

2. Materials and methodology

2.1. Materials

Polylactic acid (PLA) was provided by NatureWorks® Ingeo Co., MN,

USA (grade 2003D). Fortum (Espoo, Finland) kindly supplied lignin extracted from wheat straw (M_w-3650, M_n-1620, PDI 2, 3) using the Organosolv method. Acetic anhydride (>99%) and pyridine (99, 8%) were purchased from Sigma ALDRICH®.

2.2. Esterification

Before esterification, any moisture in the lignin was removed by drying at 50 °C for 24 h. The reaction was done in an Erlenmeyer flask, in which 50 g lignin was mixed with 150 ml acetic anhydride and 500 ml pyridine. The reaction mixture was then vigorously stirred with a magnetic stirrer for 24 h at room temperature (Hwang et al., 2022; Kim et al., 2017). The acetylated lignin solution was then added dropwise using a dropping funnel into cooled deionized water to precipitate the acetylated product. The solids were collected by vacuum filtration and were then washed five times with 500 ml deionized water until the pH of the filtrate was neutral to remove the excess pyridine and formed acetic.
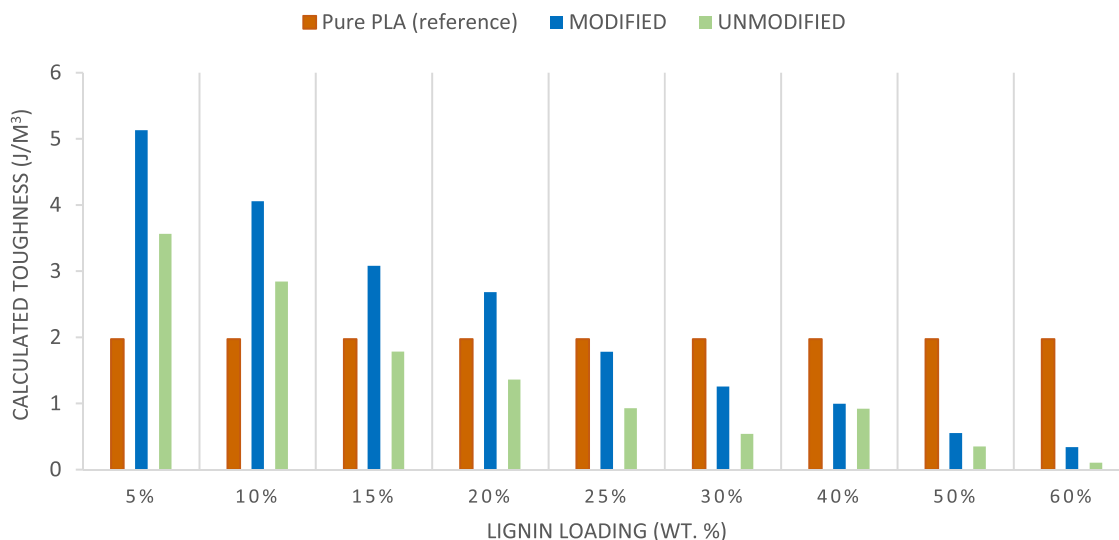
Fig. 6. Calculated toughness of the lignin/PLA blends.

Table 3

$T_{5\%}$ is the temperature correlated to 5 wt% mass loss, $T_{50\%}$ corresponds to 50 wt % mass loss. The maximal mass loss temperature (T_{D-max}) corresponds to the peak value in the dTG curve. The residuals at a fixed temperature (600 °C and 800 °C) of the unmodified and acetylated lignin are presented as char residue.

Lignin	$T_{5\%}°$C	$T_{50\%}°$C	$T_{D-max}°$C	Char residue (wt%) 600 °C	Char residue (wt%) 800 °C
Modified lignin	229	523	381	45.8	40.9
Unmodified lignin	237	542	363	46.4	42.3

The remaining solid material was finally dried in a vacuum oven (Vacucell, MMM Medcenter Einrichtungen GmbH, Munich) at 40 °C for a minimum of 24 h. Unmodified lignin was used as reference, and it was dried as described above previous to compounding and extrusion.

2.3. Extrusion of PLA/Lining blends

Prior to the blending the PLA and lignin (modified and unmodified) was oven-dried overnight at 40 °C using a vacuum oven to minimize the moisture content. Samples of modified and unmodified lignin containing 95:5, 90:10, 85:15, 80:20, 75:25, 70:30 60:40, 50:50, and 40:60 w/w were prepared. PLA and lignin were prepared and manually fed to a twin-screw microcompounder (Micro 15 cc compounder, Xplore Instruments, the Netherlands). The batch size was typically 8 g.

Processing conditions were the same for all blends from 5 wt% to 30 wt% lignin loading, 200 °C in all heating zones and the die had a temperature of 180 °C. Recirculation time was 3 min. Batches with higher lignin loading (40–60 wt%) had a recirculation time of 5 min (see Table 1). The optimum conditions had been previously determined for successful mixing of the material.

2.4. Injection molding

Specimens for the mechanical testing were then produced in an injection molding machine (Micro 12 cc, Xplore Instruments, the Netherlands) at 200 °C, and a. The mold temperature of 70 °C. The injection molding produced dumbbell shaped specimens with the size according to ISO standard 527–2 for tensile testing (Standards, 2012) and rectangular specimens for Charpy impact strength testing (80 ×10 x 4 mm) according to ISO standard 179–1 (Standards, 2010). The processing conditions for the injection-molding machine were the same for all blends (see Table 2). The samples were after removal from the mold cooled down under pressure between two metal plates to prevent deformation.

2.5. Characterization

2.5.1. Fourier transform infrared spectroscopy (FTIR)

The approximate degree of acetylation of the hydroxyl groups of the lignin was analyzed on a FTIR spectrophotometer (Nicolet iS10, Thermo Scientific, Waltham Massachusetts, US). The scans were collected in

Table 4

$T_{5\%}$ is the temperature correlated to 5 wt% mass loss, $T_{50\%}$ corresponds to 50 wt% mass loss. The maximal mass loss temperature (T_{D-max}) corresponds to the peak value in the dTG curve. The residuals at a fixed temperature (600 °C and 800 °C) of the unmodified and acetylated lignin are presented as char residue.

Unmodified lignin (UM) / Modified lignin (M)	$T_{5\%}°$C		$T_{50\%}°$C		$T_{D-max}°$C		Char residue (wt%) 600 °C		Char residue (wt%) 800 °C	
	UM	M	UM	M	UM	M	UM	M	UM	M
PLA:Lignin (w/w)										
100:0	322		359		366		0.04			
95:5	323	331	352	362	356	366	3.4	3.2	3.1	2.9
90:10	318	325	349	361	349	363	6.4	9.9	5.8	8.8
85:15	324	327	359	363	360	366	9.5	8.5	8.5	7.7
80:20	319	312	357	355	358	354	12.3	11.7	11.1	10.5
75:25	321	323	363	367	362	370	15.2	13.1	13.6	11.8
70:30	318	318	367	367	364	366	17.8	16.0	15.9	14.3
60:40	317	308	369	372	362	368	22.1	20.9	19.7	18.7
50:50	305	304	376	377	368	369	25.7	25.8	23.1	23.0
40:60	294	295	385	385	352	369	32.3	30.4	28.5	27.1

Table 5

Measured glass transition temperature of the blends containing modified and unmodified lignin.

PLA: Lignin (ratio wt %)	Glass transition temperature Modified (°C)	Standard deviation	Glass transition temperature Unmodified (°C)	Standard deviation
0:100	99.8	0.28	100.6	0.44
100:0	60.9	0.25		
95:5	60.9	0.51	60.8	0.25
90:10	60.7	0.38	60.4	0.17
85:15	60.8	0.53	60.1	0.28
80:20	60.2	0.19	59.6	0.12
75:25	60.3	0.28	59.8	0.44
70:30	59.6	0.48	59.5	0.27
60:40	59.7	0.37	59.7	0.36
50:50	59.3	0.76	58.0	0.42
40:60	59.5	0.82	56.3	0.62

absorbance mode with a resolution of 2 cm^{-1}, and over the range of 4000–400 cm^{-1}.

2.5.2. Thermogravimetric analysis (TGA)

Thermogravimetric analysis (TGA) was performed on a TGA Q500 (TA Instruments, New Castle, DE, USA). The sample size was approximately 9 mg of PLA/lignin blends, and they were analyzed at heating rate at 10 °C/min under a nitrogen from 25 °C to 900 °C. The same conditions were used for all samples. The TGA analysis will disclose the thermal decomposition phases of the sample. T_5 is the temperature correlated to 5 wt% mass loss and the maximum mass loss temperature (T_{D-max}) relates to the peak value in the derivative thermogravimetry (DTG) curve. The quantity of residue at a fixed temperature (600 °C and 800 °C) was also obtained. The weight loss curve and derivate thermograms (DTG) versus temperature were acquired from the instrument and processed using TA Universal Analysis 2000 software.

2.5.3. Differential scanning calorimetry (DSC) analysis

The glass transition temperature (T_g), the melting temperature (T_m), the degree of crystallization (X_c), and cold crystallization temperature (T_c) of unmodified and acetylated lignin was determined by differential scanning calorimetry (Q2000, TA Instruments, New Castle, DE, US). The sample size was between 5 and 10 mg, and they were analyzed under nitrogen atmosphere in standard aluminum pans (10 μL) at 10 °C/min

heating rate. Two heating scans were done, first up to 150 °C to remove interference due to moisture and previous thermal history. The samples were subsequently cooled to 25 °C and reheated to 200 °C at 20 °C/min. The results were processed using TA Universal Analysis 2000 software.

Crystallinity was calculated using Eq. 1 where ΔH_m is the measured endothermic melt enthalpy, and ΔH_c is the exothermic enthalpy that is absorbed by the crystallization during the heating. The melt enthalpy for 100% crystalline PLA used in the calculations was 93.7 J/g and is denoted as ΔH_m^∞ (Garlotta, 2001).

$$\%Crystallinity = X_c = 100\% * \frac{\Delta H_m - \Delta H_c}{\Delta H_m^\infty} \tag{1}$$

2.6. Investigation of mechanical properties

2.6.1. Tensile strength and Young's Modulus

Tensile testing was done according to the ISO 527–2 (Standards, 2012) standard test method with a Tinius Olsen H10KT Ltd. universal test machine. The specimens were loaded under 10 mm/min until breaking point. The clamping length at the start position were 25 mm. The load range was 5 kN and the presented result is an average of five replicates.

2.6.1.1. Non-instrumented Charpy impact test. The Charpy impact test was done according to the ISO 179–1 standard method (Standards, 2010) using QC-639D mechanical impact tester (Cometech testing machines, Taichung Hsien, Taiwan). The un-notched specimens were tested edgewise, and a pendulum capacity of 5 J. Five replicate samples (80 ×10 x 4 mm) were tested (Bakare, 2016).

2.6.1.2. Tensile Toughness. The toughness was determined by calculation from the area under the stress-strain curve obtained in the tensile testing using Eq. 2. The determination of toughness can be done by integration of the stress-strain curve. It is the energy of mechanical deformation per unit volume preceding fracture (Fig. 2).

$$\frac{energy}{volume} = \int_0^{\varepsilon_f} \sigma \ d\varepsilon \tag{2}$$

$U_T = Area \quad under \quad the \quad stess-strain \quad curve \quad (\sigma - \varepsilon)curve = \sigma \times \varepsilon$

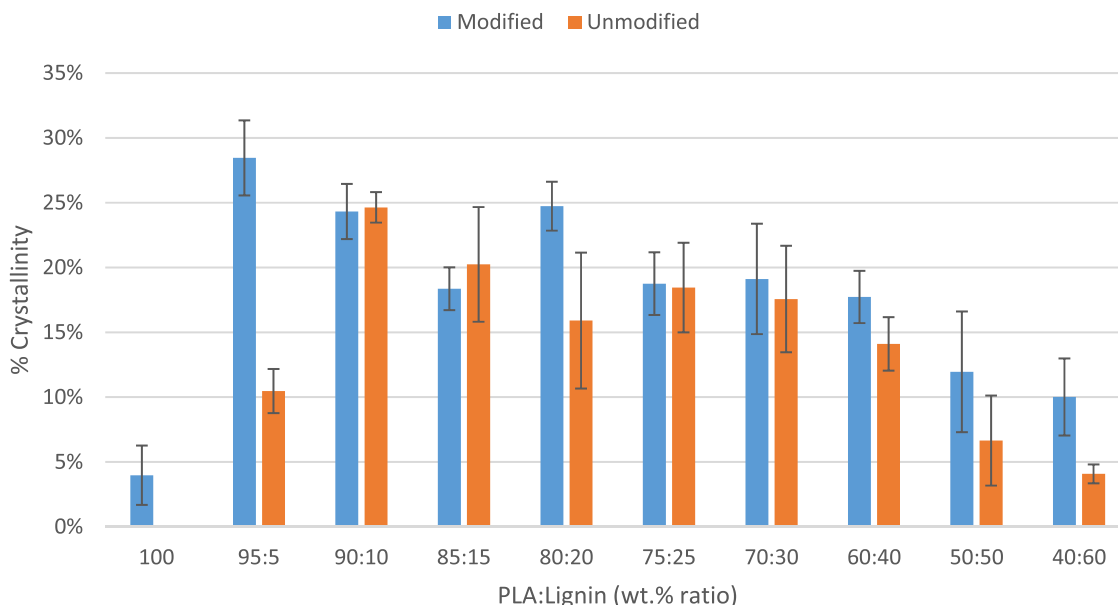$U_T \quad [=] P/A \times \Delta L/L = (N \cdot m^{-2}) \cdot (unitless)$

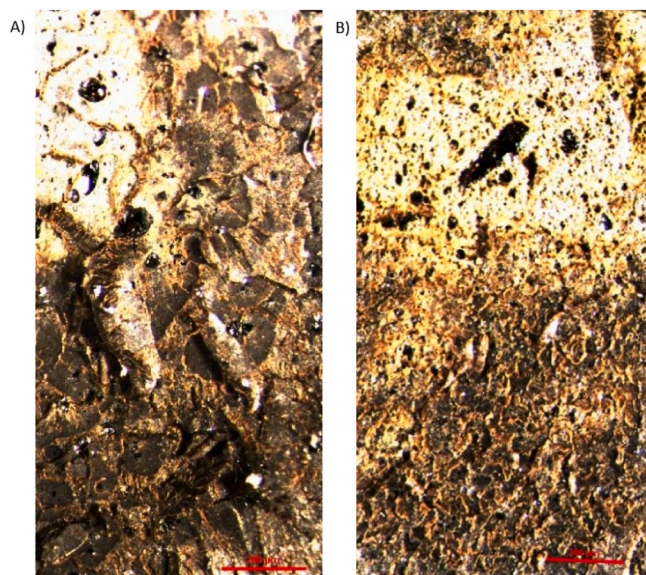**Fig. 7.** Crystallinity (percentage) of the blends containing modified and unmodified lignin.

Fig. 8. Microscopic images of A) PLA and pristine lignin (75:25 wt% ratio), and B) PLA and acetylated lignin (75:25 wt% ratio).

$$U_T [=] N \cdot m \cdot m^{-3} \tag{3}$$

where σ is stress, ε is strain, and ε_f is the strain upon failure. The toughness was calculated using Eq. 3 where U_T is the measured area under the stress-strain curve obtained by tensile testing. The data presented is an average of five samples.

2.6.2. Morphological characterization using microscopic images

Pristine and acetylated lignin blends containing 25 wt% lignin, were analyzed by an optical microscope (Nikon Eclipse LV100ND) in order to analyze the compatibility between PLA and both types of lignin. To obtain the images a cross section of the injection molded specimen were used.

2.6.3. Evaluation of moisture absorption behavior

To examine the moisture absorption behavior of the blends the PLA/Lignin specimens were conditioned in a climate chamber (HPP 108, Memmert GmbH, Germany) set to 85% relative humidity and 50 °C. Prior to placing the specimen in the climate chamber, the initial weights were determined. The specimens were taken out and weighed every 7, 14, 21, and 28 days. The reported moisture absorption was given as the percentage of the increase in weight and was calculated according to Eq. 3. The results presented are of average of five replicates (Bakare et al., 2016).

$$Percentage \quad of \quad moisture \quad absorption = \frac{W_f - W_i}{W_i} \times 100 \tag{3}$$

Where, W_f is the weight of the sample after the moisture absorption and W_i is the initial weight of the dried sample. The dry weight was obtained after drying the samples at 50 °C in a vacuum oven (Vacucell MMM GmbH, Germany) over night.

3. Results and discussion

3.1. Esterification

The chemical structure of lignin varies widely dependent on origin (softwood, hardwood, and non-wood, like wheat straw) and used extraction method (Kraft, sulfite, soda, organosolv or stem explosion). This makes the chemical structure of the lignin molecule complex (Lu et al., 2017).

Lignin was hydrophobized via esterification of its hydroxyl groups to increase the interfacial adhesion with polylactide acid (PLA) and to improve the melt-processability of the blends (Yao et al., 2021). To compare the unmodified lignin and the acetylated lignin, the samples were analyzed using FTIR. A strong intermolecular hydrogen bonding of lignin leads to self-aggregation of the lignin powder particles and uptake of moisture from the environment, which is not the case for acetylated lignin due to the replacement of the hydroxyl groups with acetyl groups that occurs during the acetylation process (Hwang et al., 2022). This makes the acetylated lignin obtain a more hydrophobic character and becomes soluble in some organic solvents.
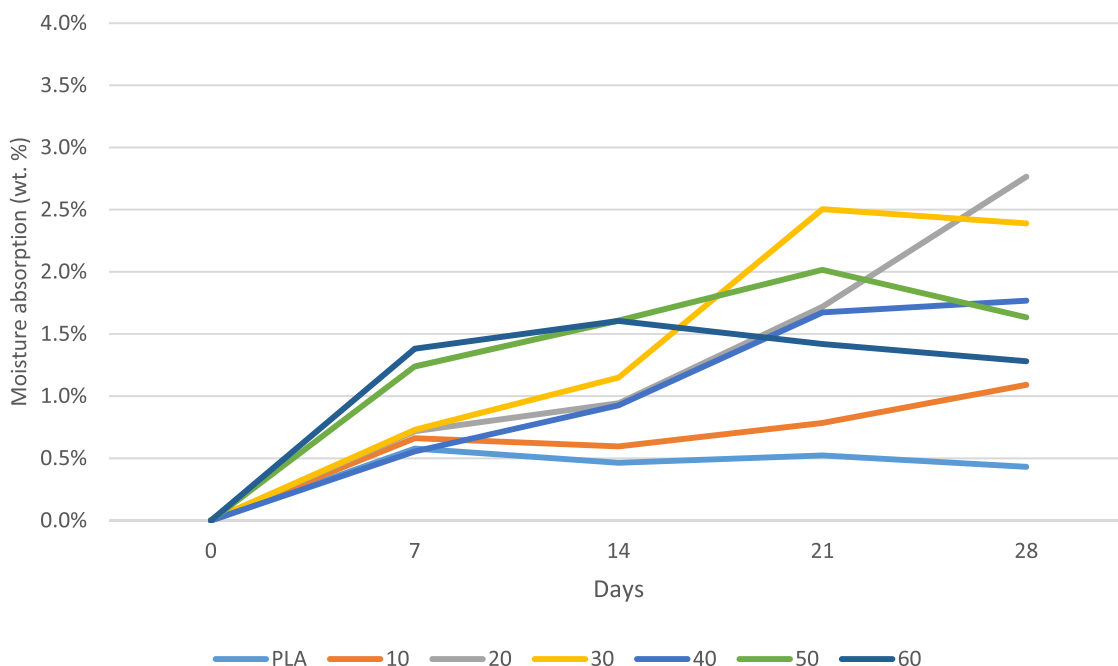

Fig. 9. Moisture absorption of the blends containing acetylated lignin and PLA from day zero to day 28 and after drying.
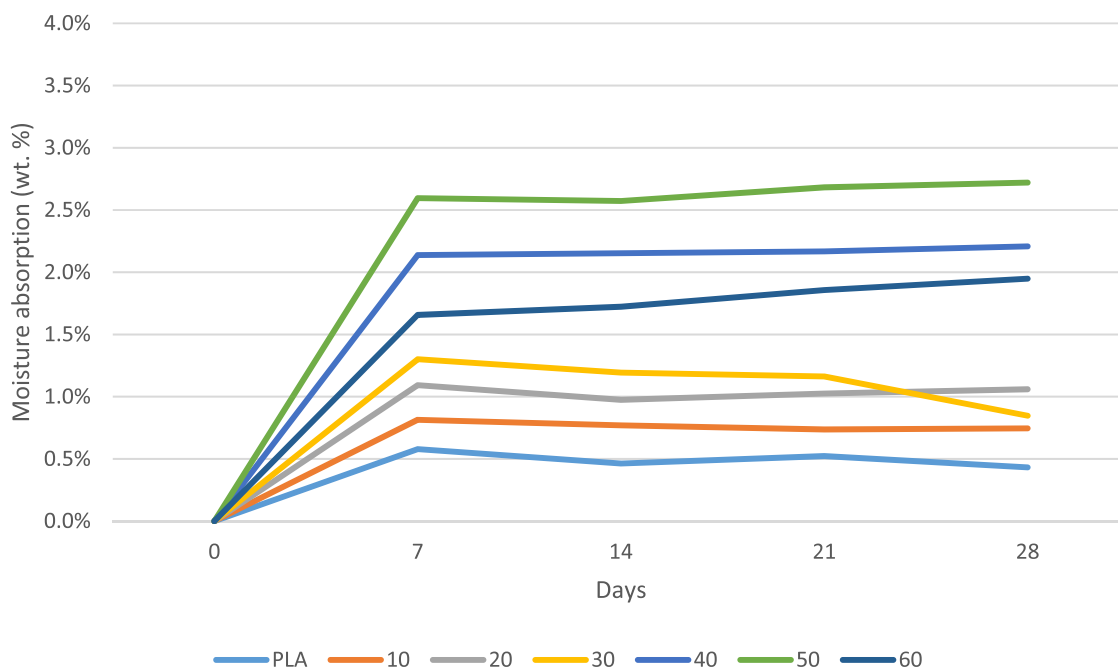
Fig. 10. Moisture absorption of the blends containing pristine lignin and PLA from day zero to day 28 and after drying.

3.2. Characterization

3.2.1. Fourier transform infrared spectroscopy (FTIR)

The wavenumbers and important bands identifications are widely represented in the literature, both for acetylated lignin, for lignin from varying extraction processes and for unmodified lignin (Delmas et al., 2011; Monteil-Rivera et al., 2013; Wang et al., 2012). Infrared spectra of the acetylated lignin samples were compared with spectra of the un-modified lignin samples to verify the extent of esterification. The spectra for the unmodified lignin displayed all characteristic lignin bands, prominently the O-H stretch at 3000–3670 cm^{-1}, the C-H stretching bands in the aromatic methoxyl groups and in the methyl, and methylene groups of side chains around 2925 and 2850 cm^{-1}.(Boeriu et al., 2004). The three absorption bands around 1600, 1510, and 1425 cm^{-1} are the characteristics of aromatic skeleton vibrations they could be observed (Fig. 1) (Guo et al., 2019; Kim et al., 2017).

The esterification reaction resulted in a radical decrease of the O-H absorption band between 3000 and 3670 cm^{-1} and the absence of absorption band in the area around 1840–1760 cm^{-1} indicated that all acetic acid anhydride is consumed in the reaction. The absence of carboxylic group band at 1700 cm^{-1} in the acetylated lignin suggests that the product does not contain any of the byproducts of acetic acid. The acetylated lignin spectra revealed three non-conjugated carbonyl groups at 1750 cm^{-1} (C=O esters), 1365 cm^{-1} (C-H bond in an –O(C=O)-CH$_3$ group), and 1195 cm^{-1} (-CO-) stretching of acetyl groups) (see Fig. 1B) (Delmas et al., 2011; In-Kyung et al., 2019; Kim et al., 2017; Monteil-Rivera et al., 2013).

3.2.2. Mechanical properties

The tensile strength results are presented in Fig. 2, and it can be observed that the tensile strength decreased with the increase in lignin load, however, the acetylated lignin showed slightly higher tensile strength at the higher loading rates in comparison to the pristine lignin. The acetylation of the lignin showed no or negligible impact on the modulus at loading rates between 5 and 15 wt% lignin.

With increased loading rate (20–30 wt% lignin), the modulus increased compared with the PLA/lignin samples containing unmodified lignin.

The modulus of the PLA/Lignin blends decreased compared with neat PLA but remained at a value of approximately 2 GPa independent of lignin loading and chemical modification (Fig. 3). However, the elongation increased in samples containing between 5 and 30 wt% lignin and a clear improvement can be observed in the samples containing modified lignin compared with the pristine lignin (Fig. 4). This could be correlated to the improvement regarding adhesion between the PLA and the lignin indicating improved compatibility (Gordobil et al., 2014).

3.2.3. Non-instrumented Charpy impact test

The energy absorbed by the Charpy impact tested samples are shown in Fig. 5. It is apparent that the modified lignin and PLA blends have a comparatively higher Charpy impact strength than the corresponding blends containing unmodified lignin and PLA. Blends containing 5 wt% lignin show a slightly higher impact strength than neat PLA. The samples containing 40–60 wt% lignin does not show a major difference in impact strength dependent on modification of the lignin. The improvement in impact strength for the blend containing modified lignin is likely due to the reduction in lignin agglomeration within the blends resulting in a more homogeneous material with higher impact resistance that is less prone to fracture.

3.2.4. Toughness

The approximate toughness of the blends was calculated using the area under the stress strain curve obtained from the tensile testing (Fig. 6). The data presented is an average of five samples. It can be observed that the calculated toughness of the blends follows the trend of the results observed in the un-notched Charpy impact tests.

3.2.5. Thermogravimetric analysis (TGA)

3.2.5.1. Lignin (acetylated and unmodified). Due to the char forming capability in combination with the thermal stability, lignin could be used as a flame retardant component in polymer blends. (Yang et al., 2020). The type and source of lignin directly determine the thermal decomposition behavior. The typical temperature of decomposition is within a range of 200–500 °C. Due to the oxygen-containing functional groups' diverse thermal stabilities and the different types of bond scissions that take place at various temperatures, the breakdown frequently

takes place over a wide temperature range. At higher temperatures, functional group cleavage, and backbone reorganization can result in the creation of high char residues, which is advantageous when considering flame retardancy.(Yang et al., 2020). The lignin used in this study undergoes upon heating a mass loss (50, 7 wt%) in the range of 200–600 °C independent of modification. The maximum heat loss rate (T_{D-max}°C) is observed at around 237 °C for unmodified lignin and at 229 °C for the modified (acetylated) lignin under nitrogen atmosphere. The outcomes indicate that the residuals of lignin remain around 46 wt% at 600 °C and around 41–42 wt% at 800 °C under nitrogen atmosphere (Table 3). Both pristine and acetylated lignin show good thermal stability and high capabilities of char-formation. Lignin could therefore be used as suitable in polymer blends for flame retardancy.

3.2.5.2. Lignin/PLA blends. The T_5% value is slight decreasing with the increase of lignin load for both modified and unmodified blends. The T_{50}% values are slightly increasing with the increase of lignin load and the maximal weight loss temperature remains fairly similar independent of lignin load, however the amount of residue increases significantly with the increase of lignin load in the blend, from around 3 wt% at 600 °C for 5 wt% lignin loads to approximately 30 wt% at 600 °C for the blend containing 60 wt% lignin. The thermogravimetric data acquired for pristine and chemically modified lignin/PLA blends are shown in Table 4. The data presented are the average number of three replicates.

3.2.6. Differential scanning calorimetry (DSC)

The most conventional method to define the thermal is by using differential scanning calorimetry (DSC). The melting and crystallization of the PLA-lignin blends was altered due to the incorporation of lignin. The DSC thermographs were used to establish the glass transition temperature (T_g) and the degree of crystallinity for neat PLA and the PLA/Lignin blends. The data from the first heating cycle was used to determine the degree of crystallinity, while the data from the second heating cycle gave the glass transition temperature. The thermal history is of high importance due to its influence on the arrangement on the amorphous and the crystalline phases and subsequently the physiomechanical properties of the material.

The glass transition temperature was established from the first endothermic peak. The second endothermic peak was used to determine melting temperature. The exothermic peak was used to determine the cold crystallization (T_c). A single glass transition temperature was detected in the DSC thermographs, which indicated a good miscibility between lignin and PLA. A slight drop in T_g could be observed when a higher lignin load than 15 wt% was introduced in the samples containing non-modified lignin and 20 wt% in the samples containing modified lignin (Table 5). It can also be observed that the trend of decreased glass transition temperature follows the increase in lignin loading, with lower observed values for blends containing unmodified lignin. The glass transition temperature for lignin varies depending on the source and quality, and can be from 90 °C to 180 °C, while the higher temperature generally corresponds to softwood Kraft lignin and the lower temperature corresponds to organosolv lignin (Feldman et al., 2001; Glasser and Jain, 1993). The glass transition temperatures of both pristine lignin and the acetylated lignin were observed at approximately 100 °C (Table 5).

The data from the initial heating scan were used to establish the degree of crystallization, by considering the melting enthalpy for 100% crystalline PLA. For the majority of the blends, a cold crystallization exothermal peak was detected before the melting endotherm peak in the heating scan. The cold crystallization peak indicated that the PLA had not reached maximum crystallization in the injection molding. A higher degree of crystallization could be achieved by a faster cooling rate after injection molding. The results indicate that the blends containing modified lignin reached a higher crystallinity compared with the blends containing unmodified lignin (Fig. 7).

3.2.7. Microscopic images

The lignin appears as dark brown spots in the white and transparent PLA domain. The size of the lignin aggregates can be related to the compatibility between lignin and PLA, which is a common trait for other polymer and lignin blends where the agglomeration decreases with enhanced interfacial adhesion. (Gordobil et al., 2014) (Kim et al., 2017). It is clear from Fig. 8 that the agglomeration of lignin particles is greater when using pristine lignin in comparison to acetylated lignin when mixed with PLA. Further it can be observed that by increasing the pristine lignin load, the agglomerates increase both in size and number compared with the acetylated lignin, this phenomena is a strong indicator of increased compatibility between the acetylated lignin and the PLA (Kim et al., 2017).

3.2.8. Water absorption behavior (Lignin/PLA blends)

Acetylation is an important modification method for lignin in order to adjust the miscibility with water. Neat PLA as a reference shows no distinct moisture absorption, which is a result of the hydrophobicity of PLA (Ren, 2010). Compared with the neat PLA, the blends displayed an increase in moisture absorption. This could be due to the chemical structure of the lignin, which tend to have a more hydrophilic character than PLA which will result in a higher moisture absorption. Since lignin has an amorphous structure one possible assumption that could be made is that the added lignin increases the molecular mobility for the structure of the blend in comparison to the tight molecular structure of neat PLA which could affect the water absorption capability (Jawaid et al., 2017). Compared with unmodified lignin, the acetylated lignin has a slightly higher initial water resistance compared with pristine lignin, which is in accordance with previous published results (Zhao et al., 2017). In this current study, it could be observed a trend of delayed moisture absorbance in the blends containing modified lignin (Fig. 9) compared with the blends containing pristine lignin (Fig. 10). This could be ascribed to the higher degree of crystallinity in the samples containing acetylated lignin since the crystalline morphology hinders the moisture absorbance and to the acetylation process of the lignin, which renders it more hydrophobic due to the substitutions of the hydroxyl groups.

4. Conclusions

The experimental work presented in this study investigated the mechanical and thermal characteristics of blends containing PLA and lignin, using both acetylated and unmodified lignin. The aim was to investigate the possibilities of utilizing lignin, which is a low-cost by-product from the pulping industry, as a matrix component in a composite to reduce the final weight and increase the non-petrochemical material usage in the composite material without compromising the thermal and mechanical performance. The esterification of lignin resulted in a high hydroxyl substitution yield and improved the interfacial adhesion between the PLA matrix and the reinforcements evidenced from the results achieved. The addition of lignin to PLA, improved the thermal stability according to the thermogravimetric analysis as well as the elongation at break under the tensile loading, and the Charpy impact strength. Microscopic images show a reduction in agglomeration of the acetylated lignin, which indicates an increased adhesion between the constituents compared with pristine lignin and PLA. Tensile strength and Young's modulus was reduced with the addition of lignin. A higher crystallinity of the material was observed in samples containing acetylated lignin in comparison with neat PLA and samples containing pristine lignin. The crystallinity of the acetylated lignin/PLA blend can be related to the delayed moisture ingress detected due to the crystal formation acting as a barrier, hindering the water molecule to penetrate the material. The result of this study indicated that acetylated lignin could be a suitable contender in the composite industry due to its many beneficial attributes and good compatibility.

CRediT authorship contribution statement

Matilda Johansson: Investigation, Methodology, Writing – original draft. **Mikael Skrifvars:** Supervision, Conceptualization, Writing – review & editing. **Nawar Kadi:** Supervision, Formal analysis. **Hom Nath Dhakal:** Supervision, Conceptualization.

Declaration of Competing Interest

The authors declare that they have no known competing financial interests or personal relationships that could have appeared to influence the work reported in this paper.

Data Availability

Data will be made available on request.

Acknowledgements

References

Agustiany, E.A., Rasyidur Ridho, M., Rahmi, D.N., Madyaratri, M., Falah, E.W., Lubis, F., Solihat, M.A.R., Syamani, N.N., Karungamye, F.A., Sohail, P., Nawawi, A., Prianto, D.S., Iswanto, A.H., Ghozali, A.H., Restu, M., Juliana, W.K., Antov, I., Kristak, P., Fatriasari, L., Fudholi, A, W., 2022. Recent developments in lignin modification and its application in lignin-based green composites: a review. Polym. Compos. 43, 4848–4865.

Anugwom, I., Lahtela, V., Kallioinen, M., Kärki, T., 2019. Lignin as a functional additive in a biocomposite: Influence on mechanical properties of polylactic acid composites. Ind. Crop. Prod. 140, 111704.

Bakare, F.O., Ramamoorthy, S.K., Åkesson, D., Skrifvars, M., 2016. Thermomechanical properties of bio-based composites made from a lactic acid thermoset resin and flax and flax/basalt fibre reinforcements. Compos. Part A Appl. 83, 176–184.

Boeriu, C.G., Bravo, D., Gosselink, R.J.A., van Dam, J.E.G., 2004. Characterisation of structure-dependent functional properties of lignin with infrared spectroscopy. Ind. Crop. Prod. 20, 205–218.

Collins, M.N., Nechifor, M., Tanasă, F., Zănoagă, M., McLoughlin, A., Stróżyk, M.A., Culebras, M., Teacă, C.-A., 2019. Valorization of lignin in polymer and composite systems for advanced engineering applications – a review. Int. J. Biol. Macromol. 131, 828–849.

Culebras, M., Geaney, H., Beaucamp, A., Upadhyaya, P., Dalton, E., Ryan, K.M., Collins, M.N., 2019. Bio-derived carbon nanofibres from lignin as high-performance Li-ion anode materials. ChemSusChem 12, 4516–4521.

Dehne, L., Vila Babarro, C., Saake, B., Schwarz, K.U., 2016. Influence of lignin source and esterification on properties of lignin-polyethylene blends. Ind. Crop. Prod. 86, 320–328.

Delmas, G.H., Benjelloun-Mlayah, B., Bigot, Y.L., Delmas, M., 2011. Functionality of wheat straw lignin extracted in organic acid media. J. Appl. Polym. Sci. 121, 491–501.

Feldman, D., Banu, D., Campanelli, J., Zhu, H., 2001. Blends of vinylic copolymer with plasticized lignin: thermal and mechanical properties. J. Appl. Polym. Sci. 81, 861–874.

Fernandes, E.M., Pires, R.A., Mano, J.F., Reis, R.L., 2013. Bionanocomposites from lignocellulosic resources: Properties, applications and future trends for their use in the biomedical field. Prog. Polym. Sci. 38, 1415–1441.

Figueiredo, P., Lintinen, K., Hirvonen, J.T., Kostiainen, M.A., Santos, H.A., 2018. Properties and chemical modifications of lignin: Towards lignin-based nanomaterials for biomedical applications. Prog. Mater. Sci. 93, 233–269.

Garlotta, D., 2001. A literature review of poly (lactic acid). J. Polym. Environ. 9, 63–84.

Glasser, W.G., Jain, R.K., 1993. Lignin derivatives. I. alkanoates.

Gondaliya, A., Nejad, M., 2021. Lignin as a partial polyol replacement in polyurethane flexible foam. Molecules 26, 2302.

Gordobil, O., Egüés, I., Llano-Ponte, R., Labidi, J., 2014. Physicochemical properties of PLA lignin blends. Polym. Degrad. Stab. 108, 330–338.

Guo, J., Chen, X., Wang, J., He, Y., Xie, H., Zheng, Q., 2019. The influence of compatibility on the structure and properties of PLA/lignin biocomposites by chemical modification. Polymers 12, 56.

Hwang, U., Lee, B., Oh, B., Shin, H.S., Lee, S.S., Kang, S.G., Kim, D., Park, J., Shin, S., Suhr, J., 2022. Hydrophobic lignin/polyurethane composite foam: An eco-friendly and easily reusable oil sorbent. Eur. Polym. J. 165, 110971.

In-Kyung, P., Hanna, S., Sung-Hoon, K., Youngjun, K., Go Eun, K., Youngkwan, L., Taesung, K., Hyouk Ryeol, C., Jonghwan, S., Jae-Do, N., 2019. Solvent-free bulk polymerization of lignin-polycaprolactone (PCL) copolymer and its thermoplastic characteristics. Sci. Rep. 9, 1–11.

Jawaid, M., Paridah, M.T., Saba, N., 2017. Lignocellulosic fibre and biomass-based composite materials: processing, properties and applications. Woodhead Publishing.

Kim, Y., Suhr, J., Seo, H.-W., Sun, H., Kim, S., Park, I.-K., Kim, S.-H., Lee, Y., Kim, K.-J., Nam, J.-D., 2017. All biomass and UV protective composite composed of compatibilized lignin and poly (Lactic-acid). Sci. Rep. 7, 43596.

Liao, J.J., Latif, N.H.A., Trache, D., Brosse, N., Hussin, M.H., 2020. Current advancement on the isolation, characterization and application of lignin. Int. J. Biol. Macromol. 162, 985–1024.

Lora, J.H., Glasser, W.G., 2002. Recent industrial applications of lignin: a sustainable alternative to nonrenewable materials. J. Polym. Environ. 10, 39–48.

Lu, Y., Lu, Y.-C., Hu, H.-Q., Xie, F.-J., Wei, X.-Y., Fan, X., 2017. Structural Characterization of Lignin and Its Degradation Products with Spectroscopic Methods. J. Spectrosc. 2017, 8951658.

Lu, Y.-C., Lu, Y., Fan, X., 2020. Structure and characteristics of lignin. Lignin: Biosynth. Transform. Ind. Appl. 17–75.

Monteil-Rivera, F., Phuong, M., Ye, M., Halasz, A., Hawari, J., 2013. Isolation and characterization of herbaceous lignins for applications in biomaterials. Ind. Crop. Prod. 41, 356–364.

Nguyen, N.A., Barnes, S.H., Bowland, C.C., Meek, K.M., Littrell, K.C., Keum, J.K., Naskar, A.K., 2018. A path for lignin valorization via additive manufacturing of high-performance sustainable composites with enhanced 3D printability. Sci. Adv. 4, eaat4967.

Parit, M., Jiang, Z., 2020. Towards lignin derived thermoplastic polymers. Int. J. Biol. Macromol. 165, 3180–3197.

Park, J.H., Kim, K.J., Lee, J.W., Yoon, J.K., 2015. Light-weight design of automotive suspension link based on design of experiment. Int. J. Automot. Technol. 16, 67–71.

Pucciariello, R., Villani, V., Bonini, C., D'Auria, M., Vetere, T., 2004. Physical properties of straw lignin-based polymer blends. Polymer 45, 4159–4169.

Ragauskas, A.J., Beckham, G.T., Biddy, M.J., Chandra, R., Chen, F., Davis, M.F., Davison, B.H., Dixon, R.A., Gilna, P., Keller, M., Langan, P., Naskar, A.K., Saddler, J. N., Tschaplinski, T.J., Tuskan, G.A., Wyman, C.E., 2014. Lignin valorization: improving lignin processing in the biorefinery. Science 344, 1246843.

Ren, J., 2010. Biodegradable Poly (Lactic Acid) Synthesis, Modification, Processing and Applications, 1st ed. 2010. ed. Springer Berlin Heidelberg, Berlin, Heidelberg.

Sameni, J., Jaffer, S.A., Sain, M., 2018. Thermal and mechanical properties of soda lignin/HDPE blends. Compos. Part A Appl. 115, 104–111.

Standards, S.If, 2010. Plastics - Determination of Charpy impact properties - Part 1: Non-instrumented impact test (ISO 179–1:2010).

Standards, S.If, 2012. Plastics - Determination of tensile properties - Part 2: Test conditions for moulding and extrusion plastics (ISO 527–2:2012).

Taleb, F., Ammar, M., ben Mosbah, M., ben Salem, R., Moussaoui, Y., 2020. Chemical modification of lignin derived from spent coffee grounds for methylene blue adsorption. Sci. Rep. 10.

Tamsilian, Y., Alvani, S., Abdolkhani, F., Moghadam, E.K., 2021. Tailored behavior of polymer matrix composite materials. In: Brabazon, D. (Ed.), Encyclopedia of Materials: Composites. Elsevier, Oxford, pp. 604–614.

Tanase-Opedal, M., Espinosa, E., Rodriguez, A., Chinga-Carrasco, G., 2019. Lignin: a biopolymer from forestry biomass for biocomposites and 3D printing. Materials 12.

Thakur, V.K., Singha, A.S., Mehta, I.K., 2010. Renewable resource-based green polymer composites: Analysis and characterization. Int. J. Polym. Anal. Charact. 15, 137–146.

Thakur, V.K., Thakur, M.K., Raghavan, P., Kessler, M.R., 2014. Progress in green polymer composites from lignin for multifunctional applications: a review. ACS Sustain. Chem. Eng. 2, 1072–1092.

Triwulandari, E., Ghozali, M., Sondari, D., Septiyanti, M., Sampora, Y., Meliana, Y., Fahmiati, S., Restu, W.K., Haryono, A., 2019. Effect of lignin on mechanical, biodegradability, morphology, and thermal properties of polypropylene/polylactic acid/lignin biocomposite. Plast. Rubber Compos. 48, 82–92.

Wang, C., Kelley, S.S., Venditti, R.A., 2016. Lignin-based thermoplastic materials. ChemSusChem 9, 770–783.

Wang, K., Bauer, S., Sun, R.-C., 2012. Structural transformation of miscanthus × giganteus lignin fractionated under mild formosolv, basic organosolv, and cellulolytic enzyme conditions. J. Agric. Food Chem. 60, 144–152.

Yang, H.T., Yu, B., Xu, X.D., Bourbigot, S., Wang, H., Song, P.G., 2020. Lignin-derived bio-based flame retardants toward high-performance sustainable polymeric materials. Green Chem. 22, 2129–2161.

Yao, J., Odelius, K., Hakkarainen, M., 2021. Microwave hydrophobized lignin with antioxidant activity for fused filament fabrication. ACS Appl. Polym. Mater. 3, 3538–3548.

Zhao, X., Huang, Z., Zhang, Y., Yang, M., Chen, D., Huang, K., Hu, H., Huang, A., Qin, X., Feng, Z., 2017. Efficient solid-phase synthesis of acetylated lignin and a comparison of the properties of different modified lignins. J. Appl. Polym. Sci. 134.

Zhu, J., Yan, C., Zhang, X., Yang, C., Jiang, M., Zhang, X., 2020. A sustainable platform of lignin: from bioresources to materials and their applications in rechargeable batteries and supercapacitors. Prog. Energy Combust. Sci. 76, 100788.